CHAPTER 155

Slit-type Breakwater; Box-type Wave Absorber

by

Shoshichiro Nagai* and Shohachi Kakuno**

ABSTRACT

A box-type wave absorber, which is composed of a perforated vertical front-wall and a perforated, horizontal bottom-wall, has been proved by a number of experiments to show lower coefficients of reflection and more distinguished reduction of wave pressures than the perforated vertical-wall breakwater.

A breakwater of composite-type, which is 1500 m long and to be built at a water depth of 10 to 11 m below the Datum Line in the Port of Osaka, is being designed to set this new type of wave absorber in the concrete caissons of the vertical-walls which is named "a slit-type breakwater". The typical cross-section of the breakwater and the advantages of the slit-type breakwater are presented herein.

INTRODUCTION

Since the papers of a perforated vertical wall breakwater were published by Jarlan (1961)[1] and Boivin (1964)[2] on the Dock and Harbour Authority, some papers on the perforated breakwater and quay-wall have been published in Britain[3] and Japan[4].

However, the physical principles in the wave attenuation of the perforated vertical breakwater has not been made clear, therefore, decisive relationships between the characteristics of incoming waves and the optimum width of the chamber have not been obtained.

EXPERIMENTAL EQUIPMENT AND PROCEDURES

All experiments concerning the bazic studies of the box-type wave absorber and the comparisons of reflection coefficient between the box-type wave absorber and the perforated vertical wall breakwater were

* Professor of Hydraulic Engineering, Faculty of Engineering, Osaka City University, Osaka, Japan.

** Research Associate of Hydraulic Engineering, Faculty of Engineering, Osaka City University, Osaka, Japan.

carried out on a model-to-prototype scale of 1/25 in a 50 m-long wave channel of 1 m-width and 1.65 m-height with one side of glass wall at the Harbour and Coastal Engineering Laboratory of Osaka City University.

The height of an incident wave, H_I, and those of composite waves, H_C, generated in front of the box-type wave absorbers and the perforated vertical wall breakwaters were measured by visual observation through the glass wall and by wave-recorders. The reflection coefficients were calculated by means of the expression $K_R = (H_C - H_I)/H_I$. Each test was repeated several times to make sure of the results. The fluctuations of the water level inside the chamber were measured by two wave-gauges and the horizontal and vertical velocities of water particles at the perforations (circular holes of 6 cm-diameter) were measured by current-meters of photo-transister-type.

The depth of water was constant 94 cm in most of the experiments in the 50 m-long wave channel, and only when the effects of the water depth and the water level on the reflection coefficient of the composite waves were investigated, the water depth was changed h = 59 cm, 72 cm, 78 cm, 86 cm, 94 cm, and 102 cm. Two groups of $H_I \cong$ 3 cm to 6 cm and $H_I \cong$ 10 cm to 14 cm were used for the incident wave height, but the period of the incident wave was widely changed T_I = 0.8 sec, 1.0 sec, 1.2 sec, 1.4 sec, 1.6 sec, 1.8 sec, 2.0 sec, 2.2 sec and 2.4 sec.

The width of the 1/25-model of box-type wave absorber, l, was changed from 16 cm to 80 cm, shown in Fig. 1. In most of the experiments the height of the models were constant 24 cm and the vertical front-wall had two rows of the perforations as shown in Fig. 1. The models of perforated vertical wall breakwaters and box-type wave absorbers were made of 4 cm-thick plywood, and most of the perforations used in the experiments were circular holes of 6 cm-diameter after the tests of the effect of the shape on the reflection coefficient, K_R. The void ratio of the perforated vertical front-wall, λ, and that of the perforated bottom-wall, λ', were widely changed from 0.00 to 0.47 to investigate the effects of λ and λ' on the K_R, but in most of the experiments λ was kept nearly constant 0.22, and $\lambda' \cong$ 0.13 or 0.15 and 0.25, as shown in Fig. 1. The small void ratios of λ' = 0.13, 0.15 and 0.17 were made by closure of the seaward half of the perforated horizontal bottom-wall of λ' = 0.25 or 0.26.

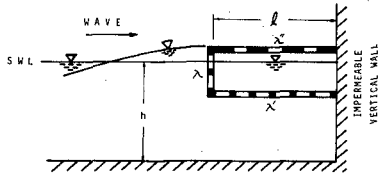

ℓ : CHAMBER WIDTH
λ : VOID RATIO OF FRONT SCREEN
λ' : VOID RATIO OF BOTTOM WALL
λ'' : VOID RATIO OF TOP WALL
h : WATER DEPTH

MODEL	ℓ	λ	λ'	λ''
MODEL 1	16 cm	0.24	0.29	0.29
MODEL 2	22 cm	0.22	0.26	0.26
MODEL 2-1	22 cm	0.22	0.17	0.26
MODEL 3	30 cm	0.22	0.25	0.25
MODEL 3-1	30 cm	0.22	0.17	0.25
MODEL 4	40 cm	0.26	0.26	0.26
MODEL 4-1	40 cm	0.26	0.13	0.26
MODEL 5	54 cm	0.22	0.25	0.25
MODEL 5-1	54 cm	0.22	0.15	0.25
MODEL 6	60 cm	0.22	0.25	0.25
MODEL 6-1	60 cm	0.22	0.15	0.25
MODEL 7	70 cm	0.22	0.26	0.26
MODEL 7-1	70 cm	0.22	0.13	0.26
MODEL 8	80 cm	0.22	0.25	0.25
MODEL 8-1	80 cm	0.22	0.13	0.25

Fig. 1. Kinds of box-type wave absorber used in the experiments

The chamber width of the perforated vertical wall breakwater was changed l = 30 cm, 40 cm and 80 cm, and the void ratio of the vertical wall was kept constant $\lambda = 0.23$.

The experiments of the slit-type breakwaters which took advantage of the box-type wave absorber have been conducted on a scale of 1/15 in a 100 m-long wave channel with a wind blower, 2 m-deep and 1.2 m-wide at the laboratory, the one side of the walls of which is made of 2 cm-thick glass plate to be able to make visual observation of the waves in front of and inside of the breakwater. The wave pressures were measured at several points of the perforated front-wall and the vertical solid back-wall of the slit-type breakwaters, as shown in Fig. 2, to be compared with the wave pressures on the solid vertical wall of the conventional composite-type breakwaters, and also the uplift pressures were measured at the bottom-wall of the box-type wave absorber. The widths of the box-type wave absorber of the slit-type breakwater, l, were changed 5.50 m and 3.75 m in prototype. The models were made of iron plates. The void ratio of the perforated vertical front-wall was $\lambda = 0.22$, and that of the perforated bottom-wall $\lambda' = 0.14$.

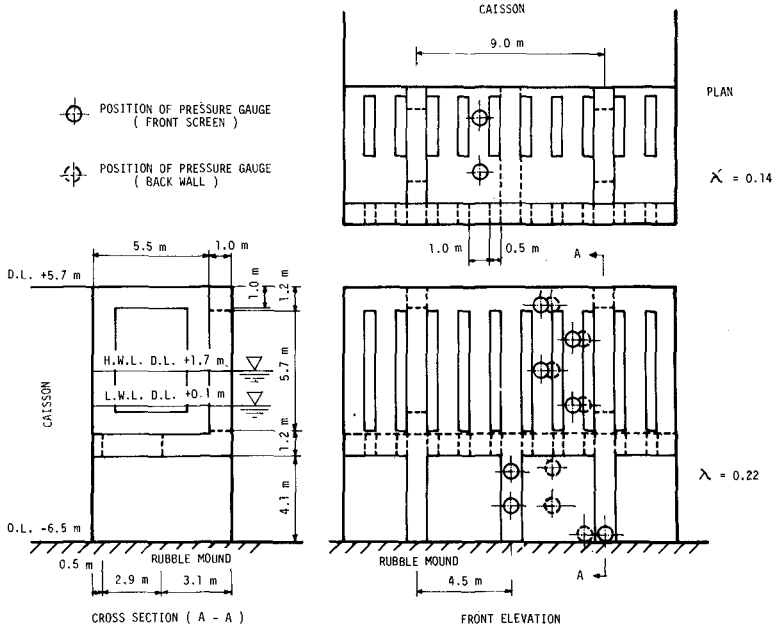

Fig. 2. Location of the wave pressure gauges

PHYSICAL PRINCIPLE OF WAVE ATTENUATION

According to the experiments and theory, which have been carried out in our laboratory, it may be stated that the wave attenuation in the perforated vertical wall breakwater is fundamentally and mainly due to the phase difference between the wave motion outside the chamber and the

fluctuations of the water level inside. As the phase difference increases, larger mass of incoming waves plunge into the chamber as jets which dissipate the energy of the waves due to turbulence inside the chamber. Energy loss due to friction created by passage of the jets through the perforations may be stated negligible small. Therefore, the shape and thickness of the wall of the perforation have few effects on the wave attenuation. But it is naturally important to select an adequate value of the percentage of the void of the perforated wall. As the coefficient of transmission, γ_T, of the perforated vertical wall or the perforated front-wall of the box-type absorber approaches to 0.62, the coefficient of reflection, K_R, of the composite waves generated in front of the perforated vertical wall or the box-shape wave absorber decreases toward zero.

If standing waves predominate in the waves in front of the perforated vertical wall, the water particles move only upward and downward or toward the sea and the land, reciprocally, but there is no mass transport which can create strong jets diffusing into the chamber. From the viewpoint of wave dynamics, it is definitively necessary that progressive waves are always predominant in front of the perforated vertical wall in order to create strong jets diffusing into the chamber. For this purpose the extension of the perforated vertical wall to the bottom or deeper portion of the water depth should be avoided lest standing waves should be predominant in the waves in front of the perforated vertical wall, and moreover it becomes much expensive in its construction cost as the depth of water becomes deep at a given site.

If a box-shape absorber composed of a perforated vertical front-wall and a perforated horizontal bottom-wall is attached near the sea surface to the impermeable vertical wall, as shown schematically in Fig. 1, incoming waves can plunge into the chamber of the box-shape absorber as a progressive wave, creating strong jets diffusing through the perforations into the chamber. Moreover, if adequate devices are made for the perforation of the horizontal bottom-wall of the box-shape absorber, the phase of the fluctuations of the water level inside the chamber would be possible to be delayed up to about 90° from the wave motion outside the chamber.

The width of the chamber, l, is also an important factor to reduce the reflection coefficient, K_R. When the ratio of l to the length of an incoming wave, L, that is l/L, is adequately selected, K_R of the composite waves in front of the perforated vertical wall or the box-shape absorber shows the minimum value. According to the experiment and theory, the perforated vertical wall breakwater showed the $(K_R)_{min}$ for l/L = 0.18, and the box-type absorber for l/L = 0.15 to 0.18.

The large phase difference, the adequate values of γ_T and l/L would be the fundamentally important factors for the box-type wave absorber.

The advantages of this wave absorber in the low coefficient of reflection and the distinguished attenuation of shock pressures exerted by breaking waves have been proved by extensive experiments.

DIFFERENCES BETWEEN THE BOX-TYPE WAVE ABSORBER AND THE PERFORATED VERTICAL WALL BREAKWATER

Although both progressive waves and partial standing waves are generated at the seaward domain of the box-type wave absorbers, the for-

mer are always predominant and plunge against the absorbers. In the box-type wave absorbers of Model 8 which has l = 80 cm, λ = 0.22 and λ' = 0.25 and Model 8-1 which has l = 80 cm, λ = 0.22 and λ' = 0.13, the wave motions outside the chamber, the fluctuations of the water levels at the sea-side and land-side inside the chamber, the horizontal velocities in the circular holes (middle hole) of the perforated vertical front-wall and the vertical velocities in the circular holes (landside) of the perforated horizontal bottom-wall were measured for various incident waves of $H_I \simeq$ 5 cm to 14 cm and T_I = 1.4 sec to 2.4 sec. The measured values for an incident wave of T_I = 1.8 sec and H_I = 12.9 cm are shown in Figs. 3 (a) and (b). Fig. 3 (a) shows the wave motion outside the chamber (thick full line), the fluctuation of the water level at the sea-side (dotted line) and that at the land-side (broken line), and the horizontal velocity of water particle in the circular hole located at the middle part of the perforated vertical front-wall (thin full line). Fig. 3 (b) shows the vertical velocity of water particle in the circular hole located at the land-side in the chamber (thin full line).

According to Fig. 3, it is known that the fluctuation of the water level at the sea-side in the chamber of Model 8-1 is delayed to a large extent from the wave motion outside the chamber. The maximum horizontal velocity of water particle of the incident wave calculated is $(u_c)_{max}$ = 24 cm/sec, and that passing through the circular hole is estimated $(u'_c)_{max} = (u_c)_{max}/0.22$ = 109 cm/sec, which is comparable with the measured maximum horizontal velocity u'_{max} = 120 cm/sec in Fig. 3 (a). The maximum vertical velocity of water particle of the standing wave of $2H$ = 20 cm generated on the vertical wall is calculated $(v_c)_{max}$ = 28 cm/sec, and that passing through the circular hole of the horizontal bottom-wall of Model 8 is estimated $(v'_c)_{max} = (v_c)_{max}/0.25$ = 112 cm/sec, which is close to the measured vertical velocity in the circular hole at the land-side in the chamber, v'_{max} = 120 cm/sec, shown in Fig. 3 (b).

It is also seen from Figs. 3 (a) and (b) that the maximum horizontal velocity measured at Model 8-1 (λ = 0.22) is u'_{max} = 130 cm/sec, which is larger than u'_{max} = 120 cm/sec measured at Model 8 (λ = 0.22), and the maximum vertical velocity measured at Model 8-1 (λ' = 0.13), v'_{max} = 80 to 110 cm/sec, is smaller than $v'_{max} \simeq$ 120 cm/sec at Model 8 (λ' = 0.25). The fluctuations of the water level at the land-side in the chamber at Model 8-1 decrease considerably compared with those at Model 8.

These facts indicate that at Model 8-1 which closes the sea-side half of the perforated horizontal bottom-wall to make λ' = 0.13, the wave motion at the loop of the standing wave generated at the vertical (non-perforated) wall is controlled considerably, and this means the suppression of the energy of the standing wave at the vertical wall which results in the increase of the horizontal velocities of the incoming wave, causing large discharges of the incoming waves plunging into the chamber, with strong jets diffusing into the chamber through the perforations. Due to this, the coefficient of reflection, K_R, of Model 8-1 decreases to 0.20 to 0.34 for larger incident waves of H_I = 10 cm to 14 cm, and moreover the values of K_R are levelled over a wide range of wave periods of 1.6 sec to 2.4 sec, as shown in Fig. 4. These characteristics of Model 8-1 would be most desirable advantages for wave absorber.

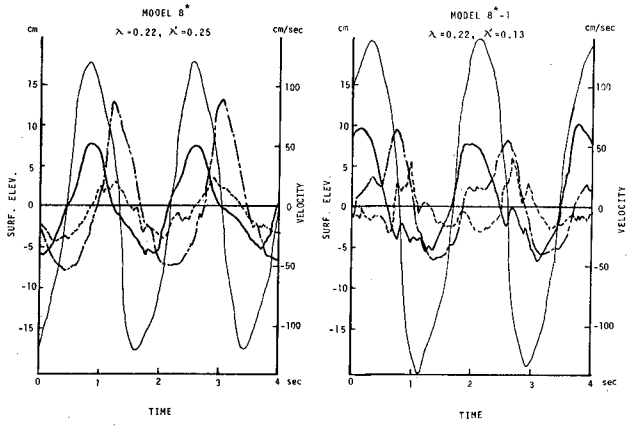

Fig. 3 (a). Horizontal velocities at the perforated horizontal front-wall

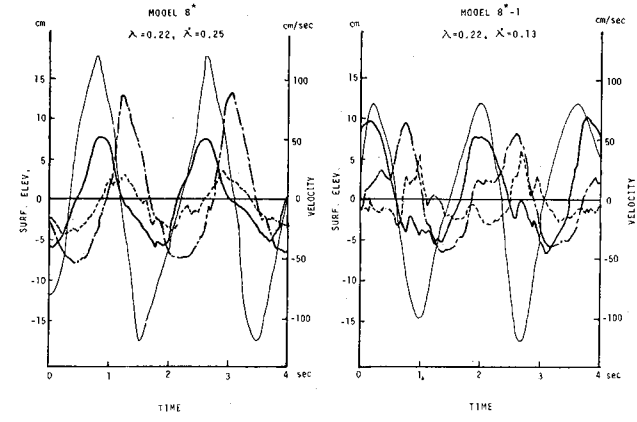

Fig. 3 (b). Vertical velocities at the perforated horizontal bottom-wall

Fig. 3. Fluctuations of the water levels inside the chamber and the curves of velocities through the circular holes

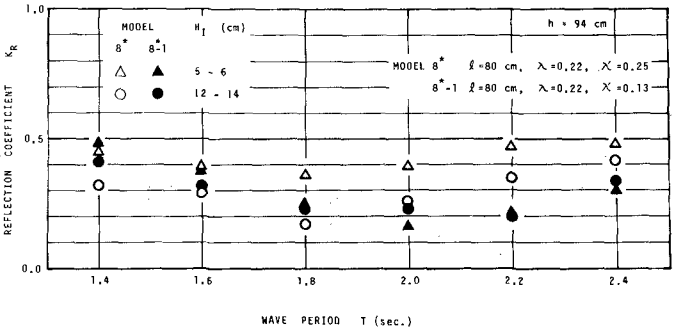

Fig. 4. Coefficients of reflection of box-type wave absorber Models 8 and 8-1

In most cases of perforated vertical wall breakwaters, standing waves with a loop at the solid vertical wall are generated at the sea-side of the perforated walls, therefore the waves do not progress towards the breakwaters, and the waves moves upwards somewhat earlier than the rising of the water level inside the chamber. This phase difference is considerably smaller than that at the box-type wave absorber described above. The horizontal velocities of water particles passing through the circular holes of the perforated vertical wall measured at the experiments were close to those calculated of standing waves generated at the solid vertical wall, and the water particles passed through the perforations towards the land and the sea, reciprocally, every a half period of the standing wave. Therefore it was observed that the discharges of the mass of the waves flowing into the chamber were smaller than those of the box-type wave absorbers, and the jets diffusing the chamber were weaker than those of the box-type absorbers. These facts resulted in larger values of K_R = 0.42 to 0.46 for incident waves with heights of H_I = 12 cm to 14 cm and periods of T_I = 1.6 sec to 2.4 sec in the Model 80 of perforated vertical wall breakwater which had a chamber width of l = 80 cm.

Fig. 5 shows the behaviours of the wave motion outside the chamber as well as the jet diffusion and strong wave spray inside the chamber when an incoming wave with H_I = 13 cm and T_I = 1.8 sec plunged against the Model 6-1 of box-type wave absorber which had chamber width of l = 60 cm, λ = 0.22, and λ' = 0.15. Fig. 6 shows the behaviours of the wave motion outside the chamber and the standing wave at the vertical wall when the same incoming wave as that of Fig. 5 came to the Model 80 of perforated vertical wall breakwater.

Fig. 5. Jet diffussion and wave spray in a box-type wave absorber

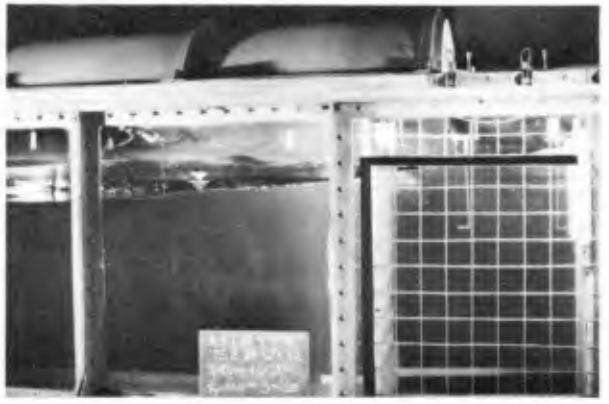

Fig. 6. Standing wave outside and inside the wave chamber of a perforated vertical wall breakwater

EFFECT OF THE VOID RATIO OF PERFORATION ON THE COEFFICIENT OF REFLECTION

(1) The void ratio of the perforated front-wall

The coefficients of reflection, K_R, for the periods T_I = 1.4 sec to 2.4 sec of incident wave are shown in Fig. 7 when the void ratios of the perforated vertical front-wall were changed λ = 0.12, 0.22, 0.30 and 0.47

at Model 8-1 which had the chamber width l = 80 cm and the constant void ratio of the perforated horizontal bottom-wall of $\lambda' = 0.13$. It is seen from Fig. 7 that K_R are at minimum values of 0.1 to 0.2 and 0.2, respectively, for $\lambda = 0.22$ and 0.30.

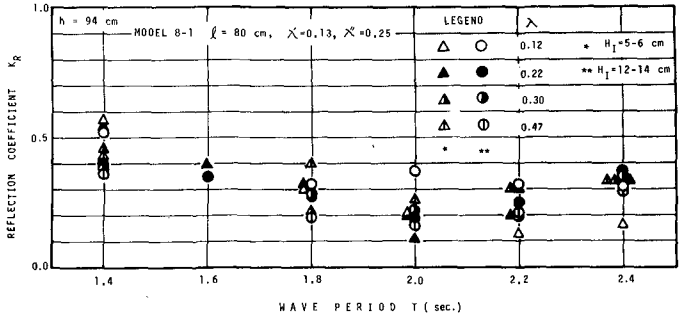

Fig. 7. Coefficients of reflection of Model 8-1 with variable λ

Fig. 8 shows the values of K_R for the different values of $\lambda = 0.00$, 0.22, 0.34 and 0.47 at Model 3 which has l = 30 cm and the constant value of $\lambda' = 0.25$. It is known that K_R also shows minimum values 0.20 to 0.24 and 0.18 to 0.37, respectively, for $\lambda = 0.22$ and 0.34.

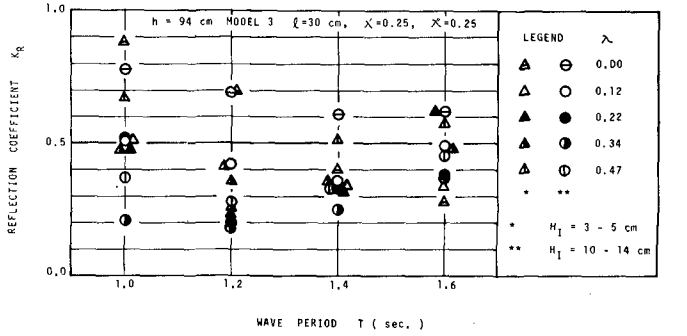

Fig. 8. Coefficients of reflection of Model 3 with variable λ

(2) The void ratio of the perforated bottom-wall

In order to investigate the effect of the void ratio of perforated horizontal bottom-wall on the coefficient of reflection, a large number of experiments were carried out by changing the values of the void ratio $\lambda' = 0.00$ to 0.43 at Model 2, 3, 4, 5, 6, 7 and 8 which all had a constant value of $\lambda = 0.22$. The experimental results showed that K_R were at minimum values of 0.10 to 0.20 for $\lambda' = 0.13$ to 0.17 where were made by closing the sea-side half of the perforated bottom-wall, Figs. 4 and 9 show the experimental results of two models of Model 8 and Model 3, respectively.

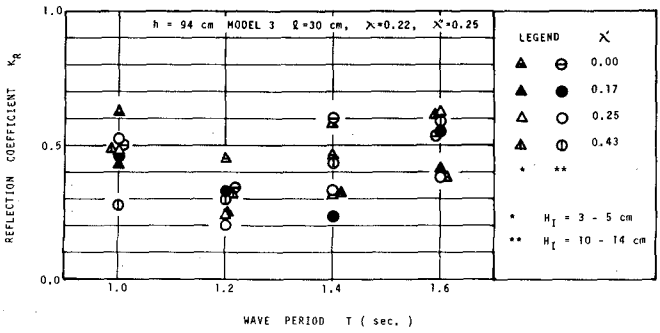

Fig. 9. Coefficients of reflection of Model 3 with variable λ'

(3) The void ratio of the top-wall

The experiments showed that the void ratio of the perforated horizontal top-wall, λ", had no effect on the coefficient of reflection if the top-wall had sufficient perforations so that it would not considerably control the upward motion of the water level inside the chamber.

THEORY

The perforated front-wall of the box-type wave absorber or the perforated vertical wall of the breakwater is situated at x = 0, shown in Fig. 10, and the vertical solid back-wall is located at x = ℓ which defines the width of the wave chamber. The incident waves incoming in the positive x direction normally on the perforated vertical wall are written

$$\eta_I = a \sin (kx - \sigma t), \qquad (1)$$

in which a = wave amplitude, k = wave number = $2\pi/L$, L = wave length, $\sigma = 2\pi/T$ and T = wave period.

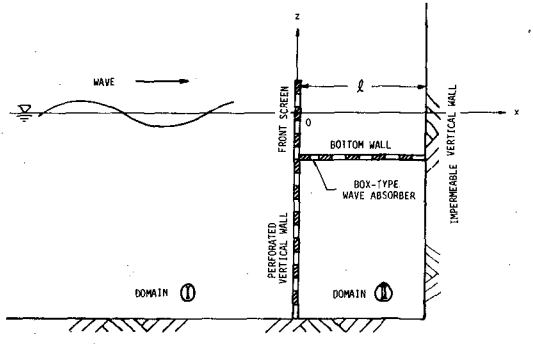

Fig. 10. Definition sketch

If the coefficient of reflection and the coefficient of transmission of the perforated vertical front-wall are denoted by γ_R and γ_T, respectively, the reflected and transmitted waves of the front-wall are written

$$\eta_R = -\gamma_R \cdot a \sin (kx + \sigma t) \tag{2}$$

and

$$\eta_T = \gamma_T \cdot a \sin (kx - \sigma t) \tag{3}$$

From the law of the conservation of mass the following relation is obtained

$$\gamma_R + \gamma_T = 1 \tag{4}$$

If η_T is supposed to be totally reflected from the solid back-wall at $x = l$ without any structure between $x = 0$ and $x = l$, the reflected wave η_{TR} is written

$$\eta_{TR} = -\gamma_T a \sin (kx + \sigma t - 2kl) \tag{5}$$

In the cases when the incident waves transmit the box-type wave absorber or the perforated vertical wall breakwater, the phase of the reflected waves from the back-wall is delayed as if a length Δl were added to the length l by passing through the perforations, and the reflected waves can be given by

$$\eta_{TR} = -\gamma_T a \sin \{ kx + \sigma t - 2k (l + \Delta l)\} \tag{6}$$

Then the composite waves generated at the sea-side of the wave absorber (shown as domain Ⓘ in Fig. 10) can be given by

$$\begin{aligned}\eta_C &= \eta_I + \eta_R + \gamma_T \cdot \eta_{TR} \\ &= a \sin (kx - \sigma t) - \gamma_R a \sin (kx + \sigma t) \\ &\quad - \gamma_T^2 a \sin \{ kx + \sigma t - 2k (l + \Delta l)\}\end{aligned} \tag{7}$$

Eq. 7 can be written

$$\eta_C = a \sqrt{A} \sin (\sigma t + \beta_1), \tag{8}$$

in which

$$\begin{aligned}A &= \gamma_T^4 + \gamma_T^2 - 2\gamma_T^3 \cos 2k (l + \Delta l) + 2 (\cos 2kx + 1)\{ 1 - \gamma_T \\ &\quad + \gamma_T^2 \cos 2k (l + \Delta l)\} + 2\gamma_T^2 \sin 2k (l + \Delta l) \sin 2kx\end{aligned} \tag{9}$$

Eq. 9 can be rewritten

$$\begin{aligned}A &= \gamma_T^4 + \gamma_T^2 - 2\gamma_T + 2 + 2\gamma_T^2 (1 - \gamma_T) \cos 2k (l + \Delta l) \\ &\quad + 2 [\gamma_T^4 + \gamma_T^2 - 2\gamma_T + 1 + 2\gamma_T^2 (1 - \gamma_T) \cos 2k (l + \Delta l)]^{1/2} \\ &\quad \times \sin (2kx + \beta_2)\end{aligned} \tag{10}$$

A takes the maximum value at $x = x_0$ where the condition of $\sin (2kx_0 + \beta_2) = 1$ is satisfied, and then $A = A_0$ is

$$\begin{aligned}A_0 &= [\{ \gamma_T^4 + \gamma_T^2 - 2\gamma_T + 1 + 2\gamma_T^2 (1 - \gamma_T) \cdot \cos 2k (l + \Delta l)\}^{1/2} \\ &\quad + 1]^2\end{aligned}$$

thus

$$\sqrt{A_0} = \{ \gamma_T^4 + \gamma_T^2 - 2\gamma_T + 1 + 2\gamma_T^2 (1 - \gamma_T) \cos 2k (1 + \Delta l) \}^{1/2} + 1 \quad (11)$$

The reflection coefficient, K_R, of the composite waves in the domain ① in Fig. 10 can be obtained by

$$K_R = \frac{a\sqrt{A_0} - a}{a} = \sqrt{A_0} - 1 = \{ \gamma_T^4 + (1 - \gamma_T)^2 + 2\gamma_T^2 (1 - \gamma_T) \cdot \cos 2k (1 + \Delta l) \}^{1/2} \quad (12)$$

Fig. 11 shows the relationships between K_R and l/L which are obtained with the parameters of $\Delta l/L$ and γ_T = 0.77 (constant). It can be seen that as the values of $\Delta l/L$ increase from 0 to 7/100, 1/10 and 1/8, the points where minimum value of K_R occurs approach from l/L = 0.25 to 0.125. Fig. 12 shows the relationships between K_R and l/L when the values of γ_T are varied from 0.1 to 0.9 at the constant value of $\Delta l/L$ = l/10. It is known that as γ_T increases from 0.1 to 0.6, K_R decreases to 0 at $\gamma_T \simeq 0.62$, and on the contrary, K_R increases again as γ_T increases from 0.62 to 0.90.

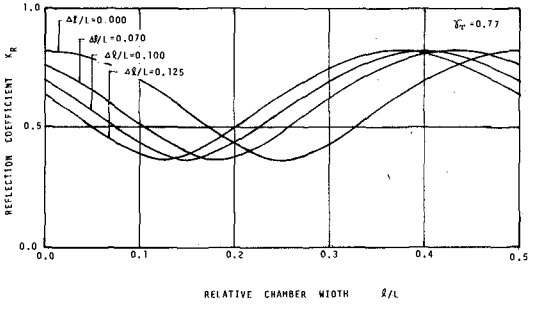

Fig. 11. Relationships between K_R and l/L with a parameter of $\Delta l/L$

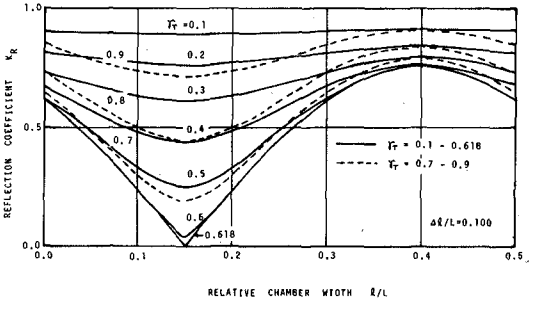

Fig. 12. Reflection coefficient dependence on γ_T

From Figs. 11 and 12, it is known that since the value of l/L where $(K_R)_{min}$ occurs decreases as the value of $\Delta l/L$ increases, it may be stated that such a wave absorber as can give as large value of $\Delta l/L$ as possible would be most favourable. Thus the maximum value of $\Delta l/L$ which can be expected as the wave absorber is obtained from the condition

$$2k\ (\ l + \Delta l\ ) = \pi \tag{13}$$

$$\left(\frac{\Delta l}{L}\right)_{max} = \frac{1}{8} \quad \text{for} \quad \frac{\Delta l}{L} = \frac{1}{L} \tag{14}$$

It may therefore be concluded that the objectives of the wave absorber are

i. the transmission coefficient γ_T should approach to 0.62, and
ii. the value of $\Delta l/L$ should approach to 1/8.

Fig. 13 shows the values of K_R for the various values of l/L measured in Models 30 (l = 30 cm), 40 (l = 40 cm) and 80 (l = 80 cm) of perforated vertical wall breakwater (λ = 0.23 = constant). The full line in Fig. 13 is a theoretical line obtained by Eq. 12, in which γ_T is taken 0.77, an average value of γ_T measured in Model 80.

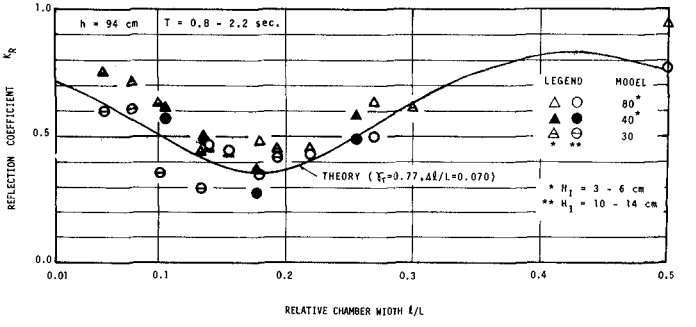

Fig. 13. Reflection coefficient dependence on l/L (perforated vertical wall breakwater)

Fig. 14 shows the values of K_R for the various values of l/L measured in Models 1 to 8 of box-type wave absorber, in which λ', the void ratio of the perforated bottom wall, are 0.13 to 0.17 except λ' = 0.29 of Model 1. The full, broken, and chain lines are all theoretical lines obtained by Eq. 12. The full line is obtained by the use of γ_T = 0.70 and $\Delta l/L$ = 0.10, and it may be stated that the full line would show the average of the experimental values of K_R when $l/L \leqq 0.15$. The chain line obtained by γ_T = 0.70 and $\Delta l/L$ = 0.07 may be said to show the average of the experimental values of K_R when l/L > 0.15, and the broken line obtained by γ_T = 0.63, the average value of γ_T measured in Model 8-1, would represent the smallest values of K_R in the vicinity of l/L = 0.15.

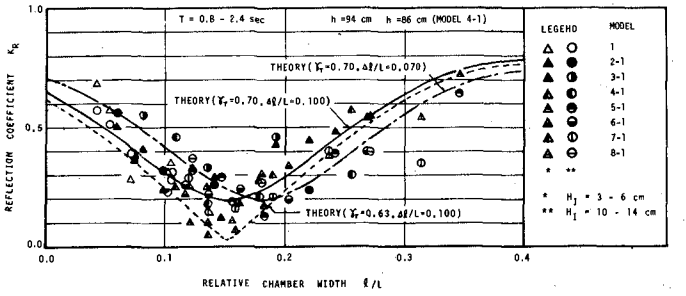

Fig. 14. Reflection coefficient dependence on l/L (box-type wave absorber)

SLIT-TYPE BREAKWATER

How to attach the box-type wave absorber to the seaward side of the caisson of breakwater and what kind of perforation would be best for the construction and structure of the caisson were discussed from the viewpoint of practical harbour engineering, and finally slits were decided as the perforations of the vertical front-wall and horizontal bottom-wall to be attached to the caisson as shown in Fig. 15.

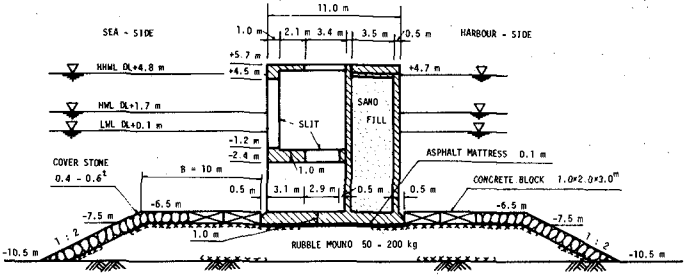

Fig. 15. Slit-type breakwater to be built in the Harbour of Osaka

All experiments to measure wave pressures exerted on the slit-type breakwaters have been carried out by generating breaking, non-breaking and standing waves by the use of models of 1/15 scale in the 100 m-long wave channel. Some of the cross-sections of the breakwaters and the characteristics of the waves used in the experiments are shown in Tables 1 and 2.

At the outset of the experiments it was confirmed that the 1/15-scale model had the same values of reflection coefficients as those in the 1/25-scale model, that is, K_R showed a minimum value of about 0.20 at waves of T = 5 sec for the breakwater of l = 5.50 m, and at T = 4 sec for the one of l = 3.75 m.

Table 1. Models of slit-type breakwater

Base rubble-mound			Water depth	
Top D.L.	Bottom D.L.	Top width B	h_1	h_2
- 6.5 m	- 10.5 m	10.5 m	6.6 m 8.2 m 9.7 m	10.2 m 12.2 m 13.7 m
- 5.0 m	- 10.5 m	10.5 m	5.1 m 6.7 m 8.2 m	10.6 m 12.2 m 13.7 m
- 5.0 m	- 10.5 m	15.0 m	5.1 m 6.7 m 8.2 m	10.6 m 12.2 m 13.7 m

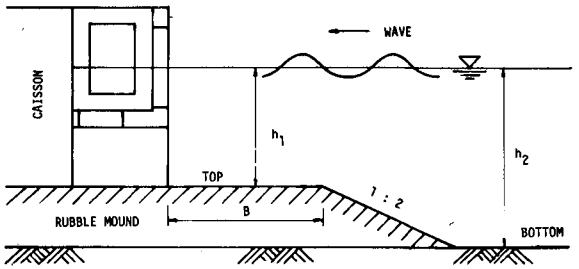

Cross-section of the slit-type breakwater model

Table 2. Characteristics of incident waves used in the experiments

Period T(sec)	Height H(m)	Length L(m)	H/L	Wind velocity V(m/sec)
10.0	4.4	95	0.046	30
8.0	4.1	72	0.057	30
7.0	4.0 to 4.3	61 to 66	0.065 to 0.069	30
7.0	3.7 to 4.3	61 to 66	0.061 to 0.065	0
6.0	3.3 to 3.4	49 to 52	0.065 to 0.067	0

The experimental results have proved that the wave pressures exerted on the slit-type breakwaters by breaking waves remarkably reduce to be less than 60 % of those on the conventional breakwaters with solid vertical caisson, and the reduction of the wave pressures becomes larger as the intensity of the shock pressure becomes higher. The upward pressures exerted on the horizontal bottom-walls are also very small. The physical reasons of the considerable reduction of wave pressures may be considered as follows.

(1) When a wave recedes from the vertical wall of the breakwater to the lowest level, the water in the chamber of the box-type wave absorber would be empty or nearly empty. Since the void ratio of the slotted bottom-wall, $\lambda' = 0.14$, is smaller than that of the slotted vertical front-wall, $\lambda = 0.22$, the phase of rising of the water level inside the chamber is delayed from the upward moving of the incoming wave outside the chamber. The shock pressure which would be exerted on the vertical front-wall by the attack of the crest of the breaking wave is remarkably reduced by diffusing through the slits into the chamber due to this retardation.

(2) Then the water level inside the chamber rises and jets diffusing through the slits of the front-wall dissipate large part of their energy by turbulence in the water inside the chamber and reduce substantially their horizontal velocities. This results in the remarkable reduction of the wave pressures on the solid vertical back-wall.

There has been no case when shock pressures were exerted by breaking waves on the front-walls and solid vertical back-walls of slit-type breakwaters even at conventional breakwaters in which shock pressures of so high intensities as 12.0 t/m^2 to 14.0 t/m^2 exerted on the vertical walls.

The wave pressures exerted on the slit-type breakwaters by standing waves were almost same as those on the conventional breakwaters with solid vertical wall.

(3) The upward pressures exerted on the horizontal slotted bottom-wall by the waves transmitted underneath the wave absorber are also as small as 1.1 t/m^2 to 2.5 t/m^2 due to the dissipation of the wave energy through the slits.

Fig. 16 and Table 3 show the comparisons of the maximum simultaneous pressures on a conventional composite-type breakwater and a slit-type breakwater.

$P_{e\ max}$ (slit) in Table 3 defines the sum of the resultants of the maximum simultaneous wave pressures exerted on the slotted vertical front-wall and that on the solid vertical back-wall. There is actually a little time difference in their occurrences, but for the safety the two maximum resultant pressures were considered to be occurred at the same time. $P_{c\ max}$ is the maximum resultant pressure calculated by the wave pressure formulas[5].

Table 3. Comparisons of max. wave pressures exerted on conventional composite-type and slit-type breakwaters

(a) Chamber width l = 5.50 m, Top of base rubble-mound D.L. - 6.5 m, Top width of base rubble-mound B = 10.5 m

Water depth h_2(m)	Incident wave: Period T(sec)	Height H(m)	Length L(m)	H/L	Composite wave height H_C (m): Solid	Slit	Coeff. of refl. K_R: Solid	Slit	Max. result. wave pressures: Solid wall $P_{e\,max}$ (t/m)	Solid wall $P_{C\,max}$ (t/m)	Slit-type $P_{e\,max}$(slit) (t/m)	Ratios of wave pressure $P_{e\,max}$ (slit) /$P_{e\,max}$	/$P_{C\,max}$	Upward pressure P_u (t/m^2)
	7.0	4.0	61	0.066	7.0	5.2	0.70	0.30	47.6*	39.1**	22.0	0.46	0.56	2.0 ∿ 2.4
10.6	7.0	3.7	61	0.061	6.5	4.7	0.78	0.29	20.4	27.1	19.1	0.93	0.70	1.8 ∿ 2.2
	6.0	3.3	49	0.067	5.8	4.2	0.74	0.27	14.9	22.0	14.7	0.99	0.67	1.4 ∿ 1.9
	7.0	4.3	64	0.067	7.3	5.5	0.74	0.31	28.1	36.9	25.2	0.90	0.68	1.8 ∿ 2.3
12.2	7.0	4.1	64	0.064	7.1	5.3	0.75	0.31	23.8	34.9	21.5	0.90	0.62	1.8 ∿ 2.1
	6.0	3.3	51	0.065	5.7	4.6	0.73	0.35	18.1	24.3	17.9	0.99	0.74	1.2 ∿ 1.5
	7.0	4.3	66	0.065	7.0	5.6	0.61	0.32	27.0	37.3	28.2	1.05	0.76	1.9
13.7	7.0	4.3	66	0.065	6.8	5.3	0.64	0.25	24.6	37.3	26.1	1.06	0.70	1.5 ∿ 1.6
	6.0	3.4	52	0.065	5.8	4.8	0.66	0.39	18.5	25.5	21.3	1.15	0.83	1.2 ∿ 1.4

* : indicates measured pressure by a breaking wave

** : indicates pressure calculated by the wave pressure formulas for breaking waves

(b) Chamber width l = 5.50 m, Top of base rubble-mound D.L. - 5.0 m, Top width of base rubble-mound B = 10.5 m

Water depth h_2(m)	Incident wave: Period T(sec)	Height H(m)	Length L(m)	H/L	Composite wave height H_C (m): Solid	Slit	Coeff. of refl. K_R: Solid	Slit	Max. result. wave pressures: Solid wall $P_{e\,max}$ (t/m)	Solid wall $P_{C\,max}$ (t/m)	Slit-type $P_{e\,max}$(slit) (t/m)	Ratios of wave pressure $P_{e\,max}$ (slit) /$P_{e\,max}$	/$P_{C\,max}$	Upward Pressure P_u (t/m^2)
	7.0	4.0	61	0.066	6.8	5.2	0.64	0.31	48.8*	49.7**	19.4	0.40	0.39	2.0 ∿ 2.4
10.6	7.0	3.7	61	0.061	6.2	5.0	0.60	0.34	36.3*	43.5**	17.5	0.48	0.40	1.8 ∿ 2.2
	6.0	3.3	49	0.067	6.2	4.3	0.82	0.30	15.9	19.1	13.4	0.84	0.70	1.4 ∿ 1.8
	7.0	4.3	64	0.067	7.2	5.5	0.64	0.27	46.5*	45.5**	28.3	0.61	0.62	1.9 ∿ 2.1
12.2	7.0	4.1	64	0.064	7.0	5.2	0.71	0.29	40.6	31.0	22.8	0.56	0.73	1.6 ∿ 2.0
	6.0	3.3	51	0.065	5.8	4.5	0.75	0.38	22.7	22.1	20.9	0.92	0.94	1.3 ∿ 1.5
	7.0	4.3	66	0.065	7.3	5.7	0.63	0.28	25.5	35.1	27.9	1.09	0.79	1.8 ∿ 2.1
13.7	7.0	4.3	66	0.065	7.2	5.7	0.66	0.35	25.4	35.1	24.9	0.98	0.71	1.8 ∿ 2.0
	6.0	3.4	52	0.065	5.9	4.5	0.72	0.35	17.7	24.9	19.8	1.12	0.79	1.0 ∿ 1.2

* : indicates measured pressure by a breaking wave

** : indicates pressure calculated by the wave pressure formulas for breaking waves

Table 3. Comparisons of max. wave pressures exerted on conventional composite-type and slit-type breakwaters

(c) Chamber width l = 5.50 m, Top of base rubble-mound D.L. - 5.0 m, Top width of base rubble-mound B = 15.0 m

Water depth h_2(m)	Incident wave Period T(sec)	Height H(m)	Length L(m)	H/L	Composite wave height H_C (m) Solid	Slit	Coeff. of refl. K_R Solid	Slit	Max. result. wave pressurss Solid wall $P_{e\,max}$ (t/m)	$P_{c\,max}$ (t/m)	Slit-type $P_{e\,max}$(slit) (t/m)	Ratios of wave pressure $P_{e\,max}$ (slit) /$P_{e\,max}$	/$P_{c\,max}$	Upward prsssure p_u (t/m^2)
10.6	7.0	4.0	61	0.066	7.1	5.6	0.77	0.31	59.8*	61.1**	33.0	0.55	0.54	2.2 ∿ 2.8
	7.0	3.7	61	0.061	6.2	5.1	0.66	0.39	47.0*	54.0**	18.5	0.39	0.34	1.8 ∿ 2.4
	6.0	3.3	49	0.067	5.9	4.3	0.81	0.33	19.6	44.7**	11.7	0.60	0.26	1.3 ∿ 1.8
12.2	7.0	4.3	64	0.067	7.2	5.6	0.64	0.30	45.6*	62.5**	24.2	0.53	0.39	1.8 ∿ 2.1
	7.0	4.1	64	0.064	6.9	5.3	0.67	0.31	26.7	31.0	20.5	0.77	0.66	1.5 ∿ 1.9
	6.0	3.3	51	0.065	5.9	4.7	0.72	0.38	16.7	22.1	19.0	1.14	0.86	1.3 ∿ 1.5
13.7	7.0	4.3	66	0.065	6.9	5.6	0.58	0.33	26.7	35.1	28.7	1.08	0.82	1.5 ∿ 1.9
	7.0	4.3	66	0.065	6.6	5.7	0.50	0.34	28.6	35.1	25.9	0.90	0.74	1.5 ∿ 1.8
	6.0	3.4	52	0.065	5.6	4.5	0.64	0.36	17.6	24.9	20.6	1.17	0.83	1.1 ∿ 1.4

* : indicates msasursd pressure by a breaking wave

** : indicates pressure calculated by the wave pressure formulas for breaking waves

(d) Chamber width l = 3.75 m, Top of base rubble-mound D.L. - 6.5 m, Top width of base rubble-mound B = 10.5 m

Water dspth h_2(m)	Incident wave Period T(sec)	Height H(m)	Length L(m)	H/L	Composite wavs height H_C (m) Solid	Slit	Coeff. of refl. K_R Solid	Slit	Max. result. wave pressures Solid wall $P_{e\,max}$ (t/m)	$P_{c\,max}$ (t/m)	Slit-type $P_{e\,max}$(slit) (t/m)	Ratios of wave pressure $P_{e\,max}$ (slit) /$P_{e\,max}$	/$P_{c\,max}$	Upward pressure p_u (t/m^2)
10.6	10.0	4.4	95	0.046	7.2	6.8	0.64	0.55	36.8	49.9	30.6	0.83	0.61	2.4
	8.0	4.1	72	0.057	7.6	6.3	0.85	0.42	52.4*	40.4**	29.4	0.56	0.73	2.3
	7.0	4.2	61	0.069	7.5	5.5	0.79	0.31	48.2*	41.6**	27.7	0.56	0.67	2.2
	7.0	4.0	61	0.066	7.0	5.3	0.70	0.34	47.6*	39.1**	20.0	0.42	0.51	1.9
	7.0	3.7	61	0.061	6.5	4.8	0.78	0.35	20.4	27.1	19.2	0.94	0.71	1.7
	6.0	3.3	49	0.067	5.8	4.5	0.74	0.43	14.9	22.0	13.2	0.89	0.60	1.5
12.2	7.0	4.3	64	0.067	7.3	6.2	0.74	0.42	28.1	36.9	26.4	0.94	0.72	1.9
	7.0	4.1	64	0.064	7.1	5.6	0.75	0.35	23.8	34.9	22.7	0.95	0.65	1.7
	6.0	3.3	51	0.065	5.7	4.7	0.73	0.44	18.1	24.3	16.2	0.90	0.67	1.2
13.7	7.0	4.3	66	0.065	7.0	6.0	0.61	0.40	27.0	37.3	30.5	1.13	0.82	1.8
	7.0	4.3	66	0.065	6.8	5.8	0.64	0.38	24.6	37.3	29.4	1.20	0.79	1.7
	6.0	3.4	52	0.065	5.8	4.6	0.66	0.38	18.5	25.5	20.4	1.10	0.80	1.1

* : indicates measured pressure by a breaking wave

** : indicates pressure calculated by the wave pressure formulas for breaking waves

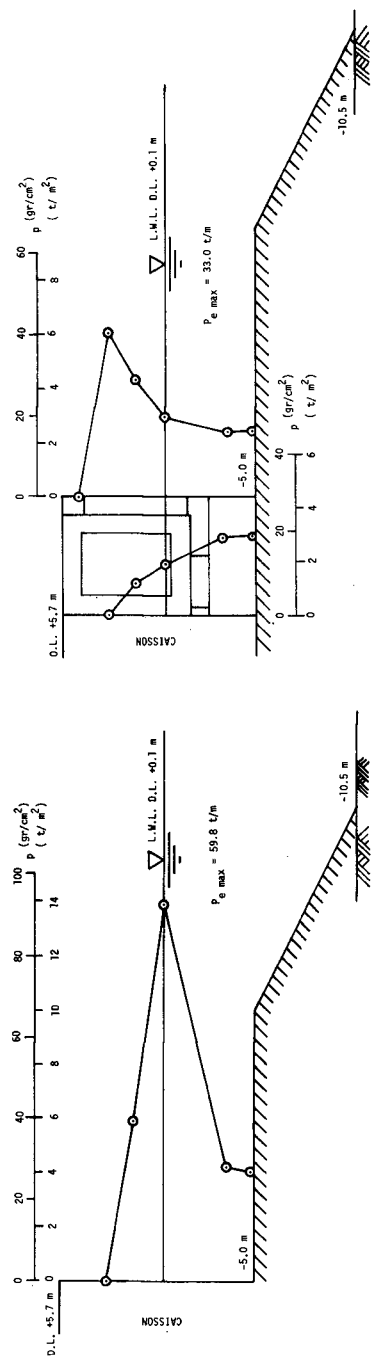

(a) T=7.0 sec, H=4.0 m, L=61 m, V=30 m/sec, H/L=0.066, $h/L=0.17$, $h_1/h_2=0.48$, $B/h_2=1.42$, $h_2/H=2.7$ SCALE=1/15

(b) T=7.0 sec, H=4.3 m, L=64 m, V=30 m/sec, H/L=0.067, $h/L=0.19$, $h_1/h_2=0.67$, $B/h_2=1.42$, $h_2/H=2.8$ SCALE=1/15

Fig. 16. Comparisons of the max. simult. pressures between conventional composite-type and slit type breakwaters (l = 5.50 m)

REFERENCES

1. Jarlan, G. E., " A Perforated Vertical Wall Breakwater ", The Dock and Harbour Authority, April, 1961, London.

2. Boivin, R., " Comments on Vertical Breakwaters with Low Coefficients of Reflection ", The Dock and Harbour Authority, June, 1964, London.

3. Terrett, F. L., Osorio, J. D. C., and Lean, G. H., " Model Studies of a Perforated Breakwater ", Proc. of the 11th Conf. on Coastal Engineering, Vol. II, Sept., 1968, London.
Marks, W., and Jarlan, G. E., " Experimental Studies on a Fixed Perforated Breakwater ", Proc. of the 11th Conf. on Coastal Engineering, Vol. II, Sept., 1968, London.

4. Nagao, G., and Kato, H., " Experimental Studies on Permeable Vertical Breakwaters ", (in Japanese), Proc. of the 17th Conf. on Coastal Engineering in Japan, 1970.
Sawaragi, T., and Iwata, K., " Some Considerations on Hydraulic Characteristics of Perforated Quay Wall ", Proc. of the Japan Society of Civil Engineers, Vol. 220, Dec. 1973.

5. Nagai, S., and Otsubo, T., " Pressures by Breaking Waves on Composite-type Breakwaters ", Proc. of the 11th Conf. on Coastal Engineering, Vol. II, Sept., 1968, London.
Nagai, S., " Pressures of Standing Waves on Vertical Wall ", Journal of Waterways and Harbours Div., Proc. of ASCE., WW1, Feb., 1969.
Nagai, S., " Pressures of Partial Standing Waves ", Journal of Waterways and Harbours Div., Proc. of ASCE., WW3, Aug., 1968.